POLITECNICO DI TORINO
Repository ISTITUZIONALE

Neutronic benchmark of the FRENETIC code for the multiphysics analysis of lead fast reactors

Original
Neutronic benchmark of the FRENETIC code for the multiphysics analysis of lead fast reactors / Nallo, G. F.; Abrate, N.; Dulla, S.; Ravetto, P.; Valerio, D.. - In: THE EUROPEAN PHYSICAL JOURNAL PLUS. - ISSN 2190-5444. - STAMPA. - 135:2(2020). [10.1140/epjp/s13360-020-00171-8]

Availability:
This version is available at: 11583/2809912 since: 2021-07-02T11:52:14Z

Publisher:
Springer

Published
DOI:10.1140/epjp/s13360-020-00171-8

Terms of use:

This article is made available under terms and conditions as specified in the corresponding bibliographic description in the repository

Publisher copyright
Springer postprint/Author's Accepted Manuscript

This version of the article has been accepted for publication, after peer review (when applicable) and is subject to Springer Nature's AM terms of use, but is not the Version of Record and does not reflect post-acceptance improvements, or any corrections. The Version of Record is available online at: http://dx.doi.org/10.1140/epjp/s13360-020-00171-8

(Article begins on next page)

19 April 2024

EPJ manuscript No.
(will be inserted by the editor)

Neutronic benchmark of the FRENETIC code for the multiphysics analysis of lead fast reactors

G.F. Nallo, N. Abrate, S. Dulla, P. Ravetto, and D. Valerio

Politecnico di Torino, Dipartimento Energia, NEMO group
Corso Duca degli Abruzzi, 24 - 10129 Torino (Italy)
giuseppefrancesco.nallo@polito.it, nicolo.abrate@polito.it,
sandra.dulla@polito.it, piero.ravetto@polito.it, domenico.valerio@polito.it

Received: date / Revised version: date

Abstract. The FRENETIC code is being developed at Politecnico di Torino in the frame of the international effort for the deployment of Lead Fast Reactor technology. FRENETIC is a multiphysics computational tool solving the neutronics and thermal-hydraulics equation at the full-core level, aiming at performing steady-state and time-dependent simulations in different conditions. In the present work, the validation activity of FRENETIC is carried forward by performing a benchmark against a reference computational model for the ALFRED design implemented in Serpent. Different core configurations in FRENETIC and different temperature distributions are considered, performing consistent comparisons between the two codes. All the results obtained show an extremely good agreement between the two models, implying that the ALFRED core can be well characterized by the FRENETIC code. The present study sets the basis for the future application of the code to simulate safety-relevant transients with FRENETIC.

PACS. 89.30.Gg Nuclear fission power – 28.50.Ft Fast and breeder reactors

1 Introduction

In the frame of the Italian activities focused on the deployment of Lead Fast Reactors (LFRs) technology, Politecnico di Torino (PoliTO) has been developing since few years a code for the multiphysics analysis of liquid-metal cooled cores, named FRENETIC (Fast REactor NEutronics/ThermalhydraulICs) [1]. The code aims at the time-dependent simulation of the neutronics (NE) and thermal-hydraulics (TH) of the reactor core, composed of closed hexagonal fuel assemblies, adopting:

- a multigroup diffusion model for neutrons, discretized with a coarse mesh nodal method at the assembly level;
- a 1D advection/diffusion model for the liquid metal flowing within each assembly, assuming no cross-flow among elements but taking into account the heat transfer between assemblies.

The models and discretization methods adopted aim at the capability to simulate in a computationally efficient way the core behavior in operational and accidental conditions. The development of the computational tool has included a wide series of validation activities (e.g. [2]), which have confirmed the capabilities of FRENETIC and have allowed to identify some necessary further developments to be included into the code, such as the inclusion of a module for the simulation of the contribution of photon gamma heat and decay heat deposition [3].

In the perspective of further validating FRENETIC, a benchmark activity has been identified, based on the comparison of the code results to a detailed reference model for a lead-cooled fast reactor, based on neutron transport, calculated with the Monte Carlo code Serpent-2 [4]. The objective is to obtain a "reference" solution for the core behavior using this extremely detailed approach and perform a comparison with the results obtained with FRENETIC in the same configuration, in order to assess its accuracy and identify possible improvements in the core modeling approximations that are part of the code structure [1]. The core design on which the study has been focused is the ALFRED LFR demonstrator [5].

The work performed in the frame of this benchmark activity allowed to obtain an optimized model of ALFRED implemented in FRENETIC, validating its accuracy also in the presence of thermal feedback effects and thus constituting an excellent starting point for the safety and stability analyses required in the development of the ALFRED design.

In this paper, after a brief introduction on the ALFRED reactor and on the FRENETIC code, the core model implemented in Serpent is described. The procedure adopted for performing space homogenization and energy collapsing of cross sections is then illustrated. The FRENETIC calculation is then compared to the Serpent calculation. The modification of the FRENETIC model following from this first comparison is presented and a second, more satisfactory NE benchmark at Hot Zero Power (HZP) is presented. Finally, results of a steady-state coupled (NE + TH) FRENETIC calculation are shown and compared with the results of a Serpent calculation adopting a consistent temperature distribution.

2 The ALFRED core

The Advanced Lead Fast Reactor European Demonstrator (ALFRED) is one of the most relevant European projects concerning the development of Lead Fast Reactors Generation-IV (Gen-IV) systems. The main objectives of Gen-IV are sustainability, long-term radioactive waste minimization, proliferation risk reduction, safety systems enhancement and cost reduction. ALFRED, which is a 300 MWth pool-type prototype system, aims at proving the LFR technological maturity, as well as assessing the LFR Small Modular Reactors (SMRs) feasibility.

With respect to commercial Light Water Reactors (LWRs), the LFR core features some advantages. Indeed, it has a higher fuel burn-up, does not require coolant pressurization and allows to increase the thermodynamic efficiency of the plant. On the other hand, due to a relevant presence of plutonium in the nuclear fuel, the neutron kinetic parameters are in general worse than for LWRs cores (i.e., leading to a faster time-dependent response), thus requiring careful evaluations of the dynamic aspects both in nominal and in accidental conditions. Due to the faster neutron kinetics, the role of thermal feedback becomes even more fundamental in order to control the reactor. For this reason, the correct simulation of the neutronics/thermal-hydraulics (NE/TH) coupling is necessary in order to assess the core performances.

The two main European countries involved in the ALFRED development are Romania and Italy. In the former, the system licensing and construction is foreseen, whereas in the latter the general design has been carried out thanks to a cooperation among industrial partners (Ansaldo Nucleare), research centers (ENEA) and universities (CIRTEN). These combined efforts have been carried out in the frame of the FP7 European project LEADER (Lead-cooled European Advanced DEmonstration Reactor) and produced the core design described in [5], which has been adopted for this work.

The core contains 171 fuel assemblies (FAs), each featuring 127 fuel pins arranged in a triangular lattice and enclosed by an external stainless steel hexagonal wrapper. Control and safety rods (CRs and SRs, respectively) are present, for the purpose of controlling the core reactivity both in normal and in accidental operating conditions. The active zone of both CRs and SRs is made of B_4C, which has been proven to be an effective neutron absorber also for fast neutrons. The central region of the core (containing FAs, CRs and SRs) is surrounded by an external reflector composed of three rings of dummy FAs (i.e., containing pins composed of zirconia). The core is surrounded by a barrel, and lead is also present in the surrouning volume, in what will be referred to as "external lead" in the following. This is cold lead coming from the pumps and flowing towards the inlet plenum (see Figure 1).

3 The FRENETIC code

The FRENETIC code [1] is aimed at performing steady-state and transient simulations of the multiphysic behavior (neutronics and thermal-hydraulics) of an LFR full core. The purpose of the tool is the simulation, during both the design and verification phases, of the core behavior in a multiphysics approach without going into detail at the pin or sub-channel level. This allows to perform simulations of several core design configurations or accidental scenarios in a short time, taking into account the feedback related to change in power, temperature or core geometry. The objective of reducing the computational time required for a simulation is thus pursued by means of simplified physics models.

The code is composed of two separate modules: the neutronic module (NE) solves the neutron flux distribution which generates the thermal power in each FA, adopting an *ad hoc* nodal method to solve the time dependent multigroup diffusion equation. The domain is discretised according to a coarse mesh structure, where the flux is

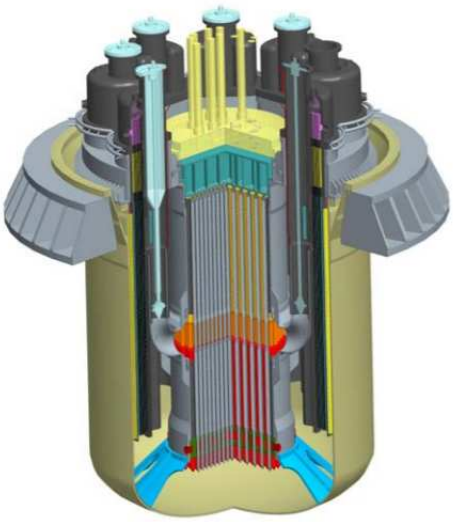

Fig. 1. ALFRED 3D sketch [6].

integrated in the considered volume to get the thermal power. The general equations system solved by this module is:

$$\begin{cases} \dfrac{1}{v_g}\dfrac{\partial}{\partial t}\phi_g(\mathbf{r},t) = \nabla\cdot(D_g(\mathbf{r},t)\nabla\phi_g(\mathbf{r},t)) - \Sigma_g(\mathbf{r},t)\phi_g(\mathbf{r},t) + \displaystyle\sum_{g'=1}^{G}\Sigma_{gg'}(\mathbf{r},t)\phi_{g'}(\mathbf{r},t) + \\ (1-\beta)\chi_g(\mathbf{r})\displaystyle\sum_{g'=1}^{G}\nu\Sigma_{f_{g'}}(\mathbf{r},t)\phi_{g'}(\mathbf{r},t) + \sum_{i=1}^{R}\chi_{g_i}(\mathbf{r})\lambda_i c_i(\mathbf{r},t) + S_g(\mathbf{r},t), \qquad g=1,\ldots,G \\ \dfrac{\partial}{\partial t}c_i(\mathbf{r},t) = \beta_i\displaystyle\sum_{g'=1}^{G}\nu\Sigma_{f_{g'}}(\mathbf{r},t)\phi_{g'}(\mathbf{r},t) - \lambda_i c_i(\mathbf{r},t), \qquad i=1,\ldots,R \end{cases} \tag{1}$$

where R delayed neutron precursor families and G neutron energy groups are considered.

The thermal-hydraulic (TH) module solves the temperature distribution according to a 1D modelling along the axial length of each FA. Neighboring FAs are weakly coupled in the radial direction by taking into account inter-assembly heat transfer. This "1D+2D" approach is inherited from the previous experience of the research group concerning the TH modeling of superconducting magnets for nuclear fusion reactors [7]. The TH module solves implicitly in time the transient 1D mass, momentum and energy balance for each FA for the z component $V(z,t)$ of the flow velocity and for the temperature of $T_{Pb}(z,t)$ and pressure $p(z,t)$ pair, in a finer spatial mesh with respect to the NE module. The detailed set of equations for this module can be found in [1].

Due to the coarser mesh along z of the neutronic module with respect to the thermal-hydraulic solver, two assumptions on the fuel and coolant temperatures are made:

1. a single averaged temperature is assumed to represent the temperature profile in each pin at the coarse mesh coordinate z_j;
2. the coolant temperature is averaged on the entire fuel assembly $x-y$ cross section.

The first statement implies the following relation:

$$T_{c,f}(z_j) = \frac{1}{L_h}\int_{z_j-L_h/2}^{z_j+L_h/2} T_{c,f}(z')dz', \tag{2}$$

where L_h is the z dimension of the NE mesh.

The coupling is achieved by exchanging, at times steps properly defined in accordance to the time scales of the phenomena, information regarding the power distribution (NE information provided to the TH module) and the temperature distribution (TH information provided to the NE module). The feedback effect is assumed linear in the form of bivariate linear interpolations on the cross section values, starting from reference data at different temperatures:

$$\Sigma(T_c,T_f) = \Sigma(T_{c0},T_{f0}) + \left(\frac{\partial\Sigma}{\partial T_f}\right)_{T_c}(T_f-T_{f0}) + \left(\frac{\partial\Sigma}{\partial T_c}\right)_{T_f}(T_c-T_{c0}). \tag{3}$$

Consequently, the generation of a set of multigroup cross sections at different fuel and coolant temperatures for each of the materials present in the reactor is required. Due to the non-linearity of the thermal-hydraulic problem, the steady-state configuration for the temperature distribution is computed in a pseudo-transient cycle, where the solution at each computational step is then passed to the NE module, see Figure 2.

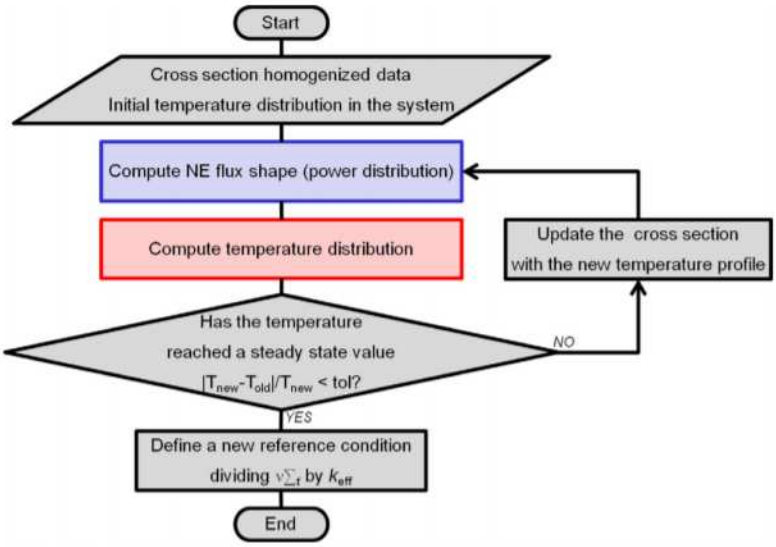

Fig. 2. Scheme for steady-state coupled calculations in FRENETIC [1].

The modules of the FRENETIC code have been validated against other computational tools and against experimental data both in stand-alone configuration [8,9] and in coupled calculations, as for the EBR-II SHRT-45R test in the frame of a Coordinated Research Project of the International Atomic Energy Agency [2].

4 Serpent-2 model of ALFRED for multigroup nuclear data evaluation

4.1 Model description

The Monte Carlo code Serpent-2 [4] is used in this work to collapse the continuous energy cross sections into six groups and to homogenise them over the reactor heterogeneous regions, thereby providing the input for the NE module of FRENETIC. Moreover, the same Serpent model is then employed as a reference to verify FRENETIC calculations. The collapsing (in energy) and homogenisation (in space) procedure is carried out by means of a detailed 3D model of the ALFRED reactor, see Figure 3. The core geometry and material compositions are consistent with the beginning of cycle (BoL) configuration (fully withdrawn control rods) provided by [5], whereas any missing data was retrieved within the framework of a collaboration with Dr. M. Sarotto from ENEA. It is worth mentioning that, during this collaboration, the correct implementation of the ALFRED geometry and material compositions in the Serpent model has been assessed by means of a benchmark against a pre-existing ERANOS model [10].

As far as the statistical convergence of the simulation is concerned, input parameters have been tuned according to convergence studies. In particular, 500 inactive cycles and 1000 active cycles have been employed, with 10^6 particle histories per cycle. These simulations settings guarantee a good fission source convergence, as shown in Figure 4. The adopted indicators were implicit and analog k_{eff} and Shannon entropy.

After a Serpent simulation has been correctly set up, suitable tallies (both in energy and in space) must be defined to generate the spatially homogenised and energy collapsed cross sections. The procedure is then repeated assuming different temperatures for coolant and fuel to reconstruct the cross section database required by FRENETIC.

4.2 Energy collapsing

As far as the energy collapsing is concerned, the calculation of effective cross sections, as well as other nuclear data, is carried out by performing an estimation of the required reaction rate on an energy interval and then dividing it by the flux average on the same interval. This ratio provides an effective cross section in that energy range that

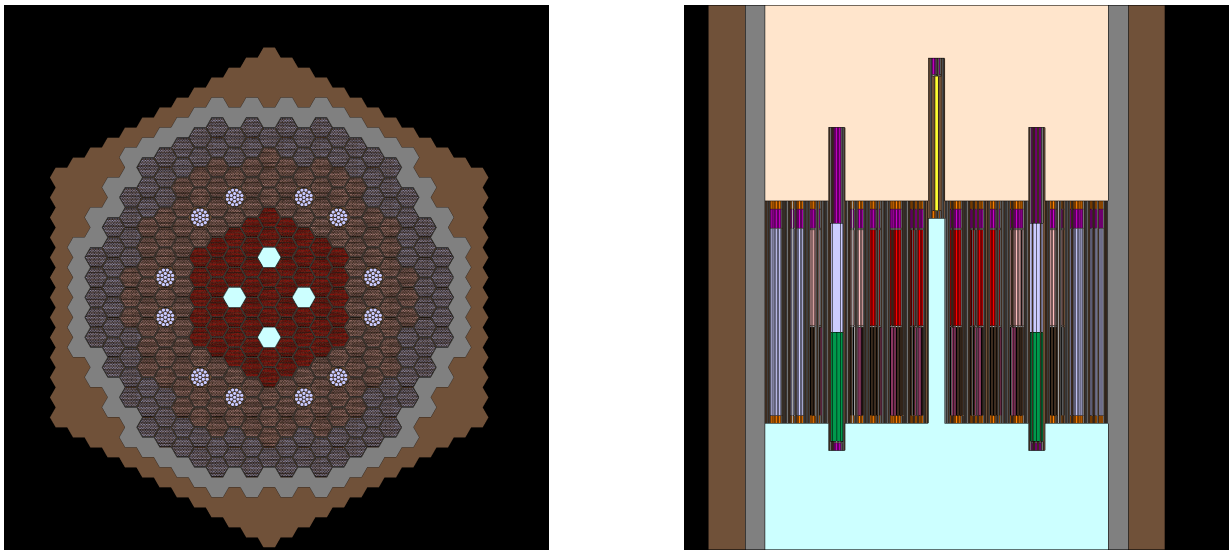

Fig. 3. Radial (left) and axial (right) view of the ALFRED configuration simulated in Serpent.

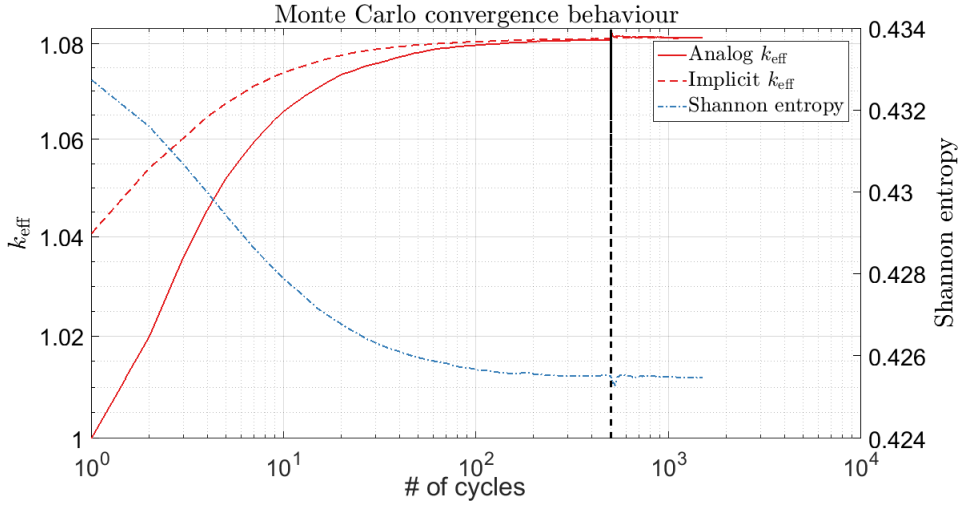

Fig. 4. Monte Carlo Serpent convergence behavior. The vertical black line indicates the boundary between inactive and active cycles.

(for an infinite medium) exactly preserves the reaction rate. The choice of the number of energy intervals and of the boundaries between them is a delicate task. For the present work, this has been performed by analysing the neutron spectra in the most important regions of the reactor core. Figure 5 reports such neutron spectra evaluated with the Serpent-2 run at 673 K. As a term of reference, in the same figure the flux subdivisions previously adopted in [11] have been introduced. A limitation of that energy discretiation is evident: the fifth group, with upper energy bound at around 10^{-2} MeV, is able to describe the neutron behavior in the fuel regions, but it appears inadequate for the description of the outer regions. In fact, the presence of a larger portion of thermalized neutrons in the reflectors and dummy elements is completely disregarded if a single energy group is assumed down from 10^{-2} MeV. To fix this issue, an additional energy group has been added, considering that six groups are sufficient to approximate the behavior of the energy distribution within the various materials. The resulting energy group boundaries are reported in Table 1.

4.3 Spatial homogenization

The energy collapsed cross sections need to be homogenized on spatial regions consistently with the structure of the FRENETIC code (i.e., homogeneous on the hexagonal fuel assembly and axially heterogeneous according to the neutronic coarse meshing). Starting from the core modeling in Serpent as detailed in Figure 3, some regions (specifically the ones far from the fission source) have been merged into a single universe for the cross section tally, in order to

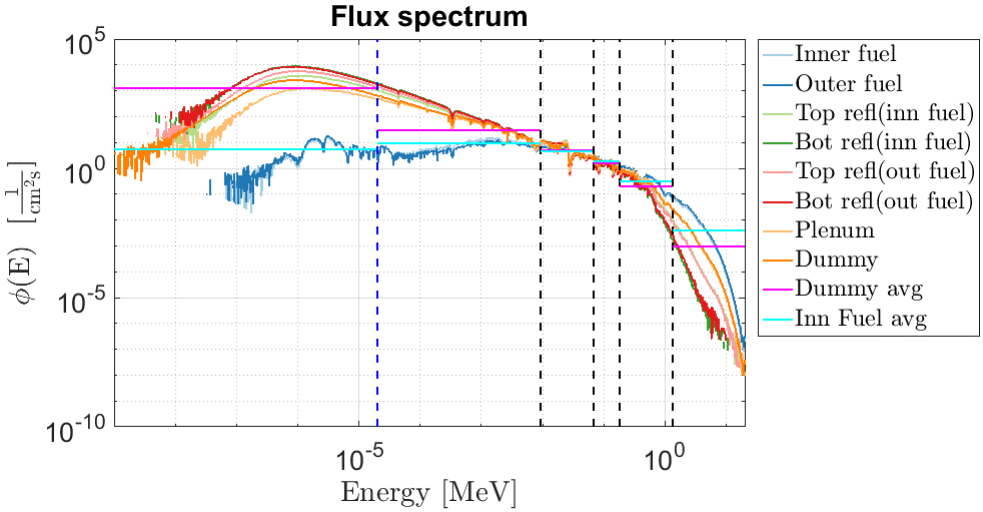

Fig. 5. Neutron flux spectra computed by Serpent for selected regions of the core. Black dashed lines identify the 5-group energy subdivision previously adopted, while the blue dashed line identifies the additional group added to better account for the reflector spectrum.

Table 1. Six-group data adopted to perform the macroscopic cross section energy collapsing and spatial homogenization.

Group	Upper boundary [MeV]	Lower boundary [MeV]
1	$2.000 \cdot 10^{1}$	$1.353 \cdot 10^{0}$
2	$1.353 \cdot 10^{0}$	$1.832 \cdot 10^{-1}$
3	$1.832 \cdot 10^{-1}$	$6.738 \cdot 10^{-2}$
4	$6.738 \cdot 10^{-2}$	$9.119 \cdot 10^{-3}$
5	$9.119 \cdot 10^{-3}$	$2.000 \cdot 10^{-5}$
6	$2.000 \cdot 10^{-5}$	$1.000 \cdot 10^{-11}$

achieve a better statistics. In particular, the external lead (in green in Figure 6), the barrel (in light grey) and the dummy element region (in dark grey), are each considered as three unique radial regions. Moreover, the 12 control rods are grouped together as a single detector. The same choice has been made for the 4 safety rods. For the inner fuel (IF) region, instead, it has been assumed that cross sections averaged on a subset of FAs (indicated in magenta in Figure 6) could be representative of the entire zone. The same strategy has been adopted for the outer fuel (OF) region, for which the representative FAs are indicated in red. It should be noticed that fuel assemblies considered for the homogenization are the ones surrounded by other assemblies of the same kind. This choice was based on a compromise between a homogenization over the whole inner and outer fuel rings and an assembly-wise homogenization, which would certainly provide a higher but probably unnecessary detail level. The few-group cross sections evaluated

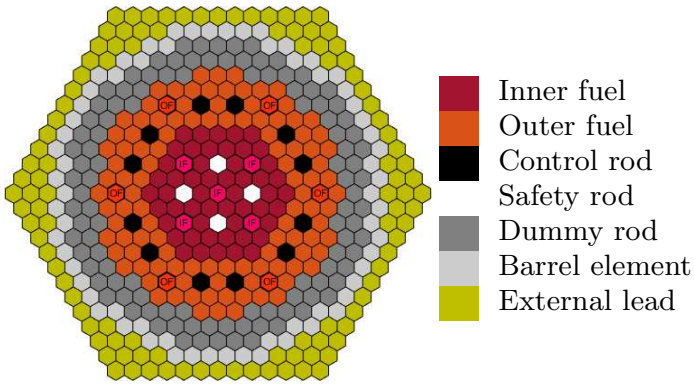

Fig. 6. Radial arrangement of the regions adopted for the cross sections homogenisation.

by Serpent have been at first homogenized axially according to the finest achievable discretization, which takes into

account all the different regions of the model, as shown in Figure 7. However, the axial discretization employed for the FRENETIC calculation is in general different -and possibly coarser- with respect to the one introduced into the transport simulation. This is due to the requirement of avoiding excessively optically thin regions, which would hinder the convergence of the nodal method employed for the spatial solution of the diffusion problem in FRENETIC [12]. Each of the coarse axial regions defined in the FRENETIC model requires a single spatial value for the multigroup cross section, which should therefore be mapped to the ones computed by the transport model for the fine subdivisions composing that coarse axial region. This is performed by means of a suitable spatial homogenization procedure, which is carried out in such a way as to preserve the reaction rate for each material.

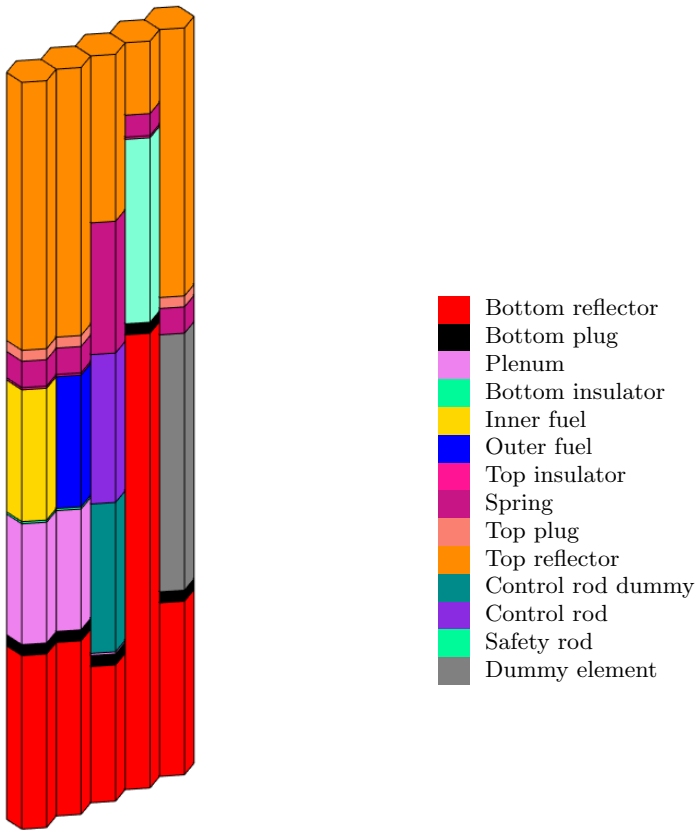

Fig. 7. Serpent axial discretisation for each radial region.

The re-homogenisation process leads to the calculation of a new set of cross sections that are averaged on the flux of each material in the "macro-region", i.e., in the FRENETIC axial mesh. Since the flux tallies calculated by Serpent are integrated on the entire volume of each material and collapsed on the energy grid division, there are six values of integrated flux in the volume where the specific material lies, as well as the cross section. The spatial homogenization is then performed according to the following formula (for the $i-$th axial mesh of a given FA):

$$\tilde{\Sigma}_{g,i} = \frac{\int_{V_i} d\mathbf{r} \bar{\Sigma}_g(\mathbf{r}) \bar{\phi}_g(\mathbf{r})}{\int_{V_i} d\mathbf{r} \bar{\phi}_g(\mathbf{r})} \approx \frac{\sum_{i=1}^{N} \left(\bar{\Sigma}_{g,i}(r) \bar{\phi}_{g,i}(r) h_{serp} \right)}{\sum_{i=1}^{N} \left(\bar{\phi}_g(r) h_i \right)} \tag{4}$$

where h_i is the axial length of the FRENETIC mesh and h_{serp} is the length of the j-th Serpent axial region which falls within the i-th axial mesh of FRENETIC. The index j goes from 1 to N, where N is the total number of materials (i.e., Serpent regions) localized in the i-th axial region of the FRENETIC mesh. From the mathematical point of view, the integration should be performed on the correct volume where the homogenization takes place, but since the transport model gives a single value of the group-averaged flux for each material, it was assumed that the integrated

Table 2. Temperatures values adopted for the Serpent runs used to evaluate the few-group cross section.

T_{fuel} [K] \ $T_{coolant}$ [K]	673	1073	1473
673	×		
1073	×	×	
1473	×	×	×

flux was simply proportional to the axial length. This means that the flux for the g-th group is averaged as if it was constant over the volume.

4.4 Temperature dependence of cross sections

The process in Serpent outlined above have been performed several times, changing the temperature of the lead coolant and of the fuel, while the temperature of the structural materials has been specified in Serpent according to the arithmetic average of the coolant and fuel temperatures. The necessity of this process is associated to the fact that the FRENETIC code evaluates the thermal feedback by interpolating cross sections between at least two temperatures according to the local temperature of the fuel and coolant. The fuel and coolant temperatures considered for the generation of this cross section library are listed in Table 2. The table lower triangular layout is due to the fact that the fuel temperature is always greater than the coolant one, at least for the reactor operational relevant scenarios for the present work.

5 Steady-state results of the FRENETIC model for the ALFRED reactor

5.1 FRENETIC NE calculations at fixed temperature

The nuclear dataset obtained by means of the procedures outlined in the previous section has been employed as input to the neutronic model of the FRENETIC code. Such dataset is distributed according to the radial "zoning" presented in Figure 8. The axial "macro-regions" indicated in Figure 7, which are each characterized by a single spatial value of the cross sections, are then subdivided into a number of sub-nodes which is sufficient to ensure the grid independence of the flux solution.

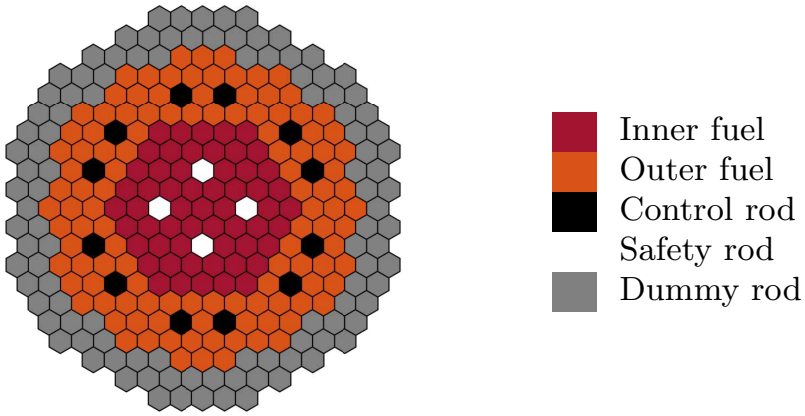

Fig. 8. Radial scheme of the FRENETIC model of the ALFRED core.

The model has been tested against a reference result in steady-state, represented by the same Serpent calculations which were performed for the generation of the cross section dataset. The benchmark has been performed by imposing the same thermal power of 300 MWth and corresponding boundary conditions for the two calculations (i.e., the transport calculation performed in Serpent and the coarse-mesh diffusion calculation performed in FRENETIC). Since this benchmark is only intended to verify the correct behavior of the NE module, the temperatures of all the materials in the core in FRENETIC have been set at 673 K, running the NE module of FRENETIC in standalone

mode. It is also worth mentioning that, although a photon transport model is now available in FRENETIC [3], it has been turned off for the purpose of guaranteeing a fair comparison between the two simulations. It must be noticed that the core modelled in FRENETIC (Figure 8) includes all elements where lead is flowing, thus excluding the barrel and dummies. This limitation is due to the fact that the TH module is not able to simulate assemblies with stagnant lead nor solid elements such as the barrel. This limitation is however fictitious at this stage, since the code is running in NE standalone, and it will be relaxed at a second stage.

The effective multiplication eigenvalue computed by the two codes is first compared. Serpent estimate is 1.08122± 3 pcm, whereas FRENETIC provides a k_{eff} equal to 1.07673, showing a rather good consistency (Δk_{eff} = 449 pcm). The radial distribution of the fission power source computed by the two codes is compared in Figure 9. The choice of comparing this quantity is physically significant, since the power source represents the exchange variable from the NE module to the TH module in multiphysics simulations. A qualitative comparison confirms that the FRENETIC code is able to reproduce the radial power distribution: for instance, for the BoL configuration here considered, the maximum value of the power per FA is not located at the core center, but at the beginning of the outer fuel zone, which is more enriched. This peculiar aspect is correctly recovered by FRENETIC as compared to Serpent.

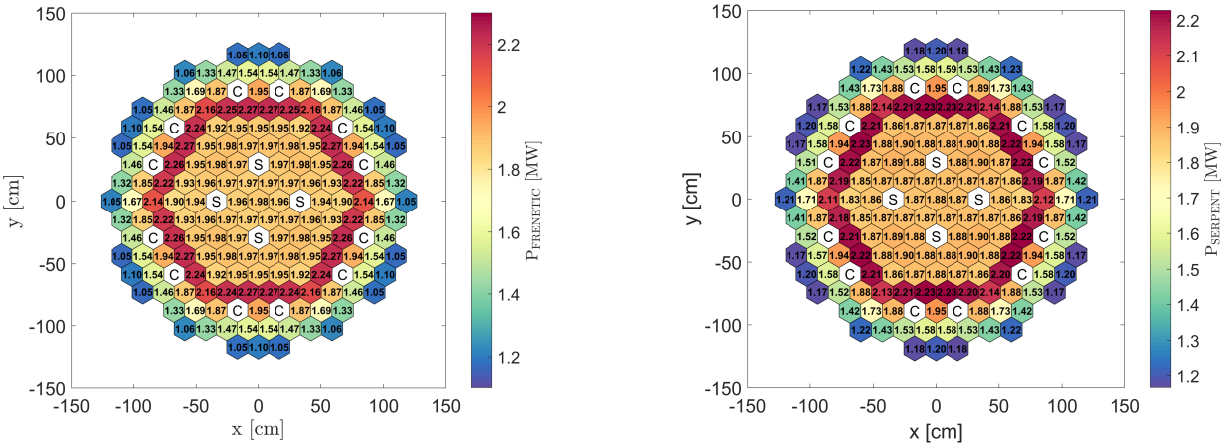

Fig. 9. Radial power map (in MW per FA) computed by FRENETIC (left) and Serpent (right).

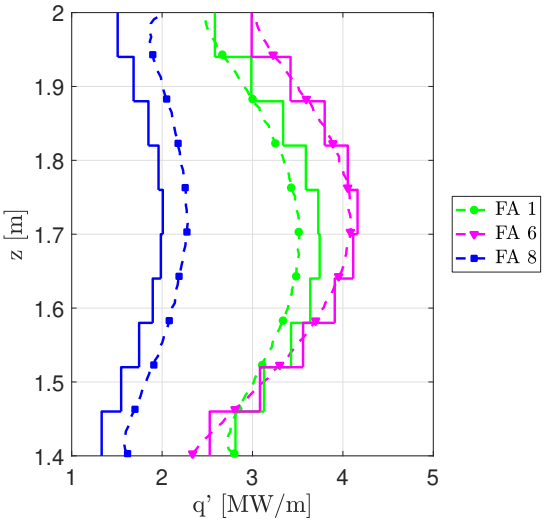

Fig. 10. Comparison between the linear power calculated by Serpent and FRENETIC for three selected FAs. Identification of FAs as in Fig. 12.

A more systematic comparison is shown in Figures 10 and 11. In particular, Figure 10 shows the axial distribution of the computed linear power for FA 1, 6 and 8 and Figure 11 a map of the relative error between the power per FA computed by the two codes. The relative difference rather than its absolute value is here presented, since this

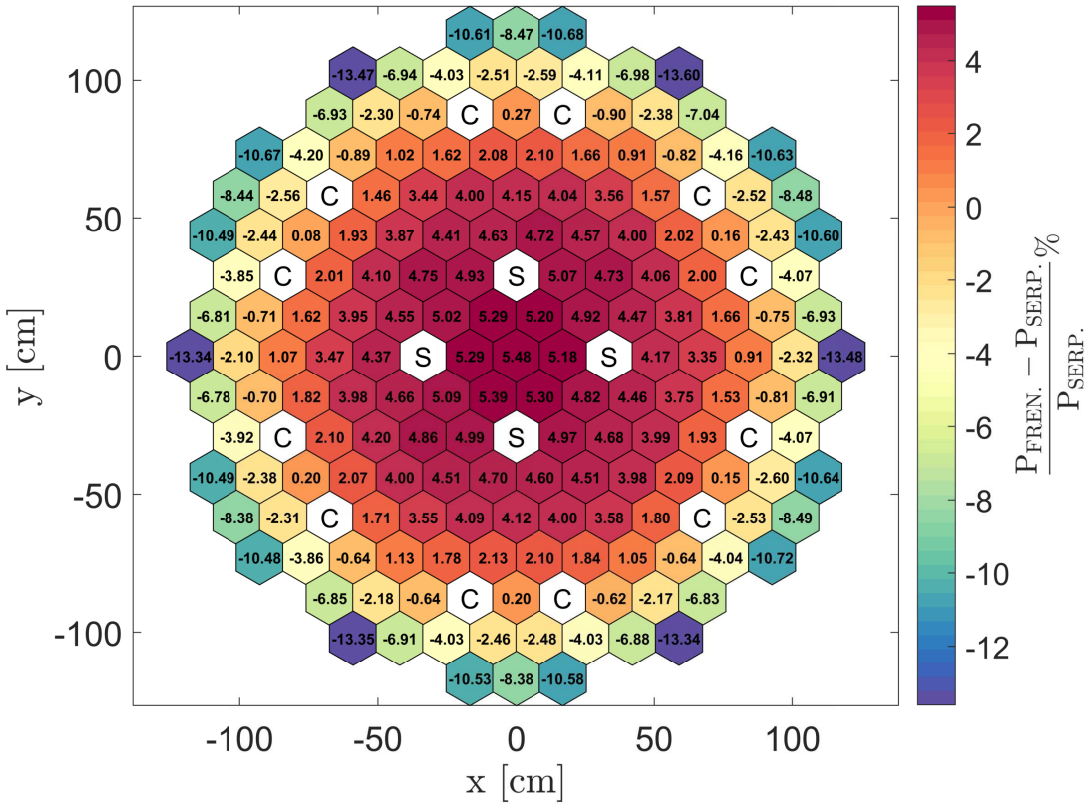

Fig. 11. Radial map of the relative error between the power per FA computed in FRENETIC and in Serpent.

choice allows to highlight the fact that FRENETIC overestimates the power per FA at the core center, whereas it underestimates it for the FAs which are located at radially outer positions. This effect is clearly visible if a comparison along a radial direction through the core is performed, as can be seen in Figures 12 and 13. These radial distributions of the relative error have suggested that the problem was in the different extension of the domain between the two models (i.e., absence of barrel and external lead in the FRENETIC model), partly explaining the different multiplication constants between the two calculations.

Other possible reasons for this discrepancy are the space homogenisation and the energy collapsing of nuclear data. To distinguish among these effects, the FRENETIC model for ALFRED has been improved by introducing the barrel and dummy elements, bearing in mind that this extended computational domain is feasible for NE calculations but suffers the limitation of the TH module. This has been achieved by adding fictitious FAs corresponding to the latter two regions, see Figure 14. These FA are fictitious in the sense that they do not participate to the TH behaviour of the code, but are accounted for by the NE model by means of suitably generated nuclear data. In this way, the radial "zoning" of the core has been made fully consistent with the one employed in the Serpent model. In Figure 15 the radial and axial heterogeneity of the ALFRED core as introduced in the FRENETIC code is shown.

The comparison between the effective multiplication eigenvalue computed by the two codes already outlines the higher fidelity of this improved model to the Serpent reference. In particular, the value computed by FRENETIC (k_{eff} = 1.08194 as opposed to the previous value of 1.07673) is in very good agreement (72 pcm difference) with the 1.08122 ± 3 pcm evaluated by Serpent. The results of the FRENETIC neutronic run for the improved ALFRED model show, as expected, that the relative error on the computed power has been greatly reduced by taking into account the presence of the barrel and of the lead outside the barrel, as can be seen in Figure 16 for what regards the linear power. In Figure 17 the relative error on the power produced per FA is reported, together with the statistical uncertainty of the Serpent results, which of course increases when moving from the center to the periphery of the core. Comparing Figure 17 with Figure 11 the improvement in the power reproduction is clearly visible. Radial distributions are provided in Figures 18 and 19, confirming the previous observation. The remaining source of errors, however rather limited, is to be attributed to the energy collapsing or spatial homogenization procedures carried out to generate the dataset for FRENETIC. In particular, to address the energy collapsing issue, one possible approach could be to improve the choice of the few energy groups through the use of optimization methods based on genetic algorithms [13]. Moreover, a more careful choice of the tallies might ensure higher fidelity in the description of the radial composition of the core.

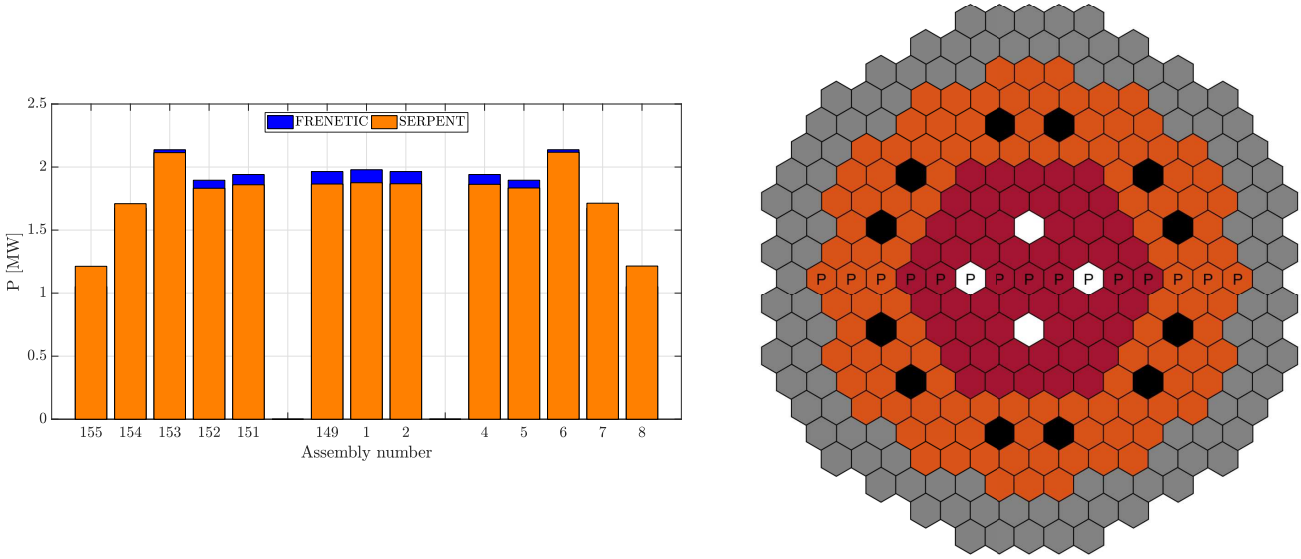

Fig. 12. Comparison between the radial power profile calculated by Serpent and the first FRENETIC model (without barrel and external lead) for some selected FAs in HZP, i.e., uniform 673 K (left), and radial map of the core with the employed FAs indicated (right).

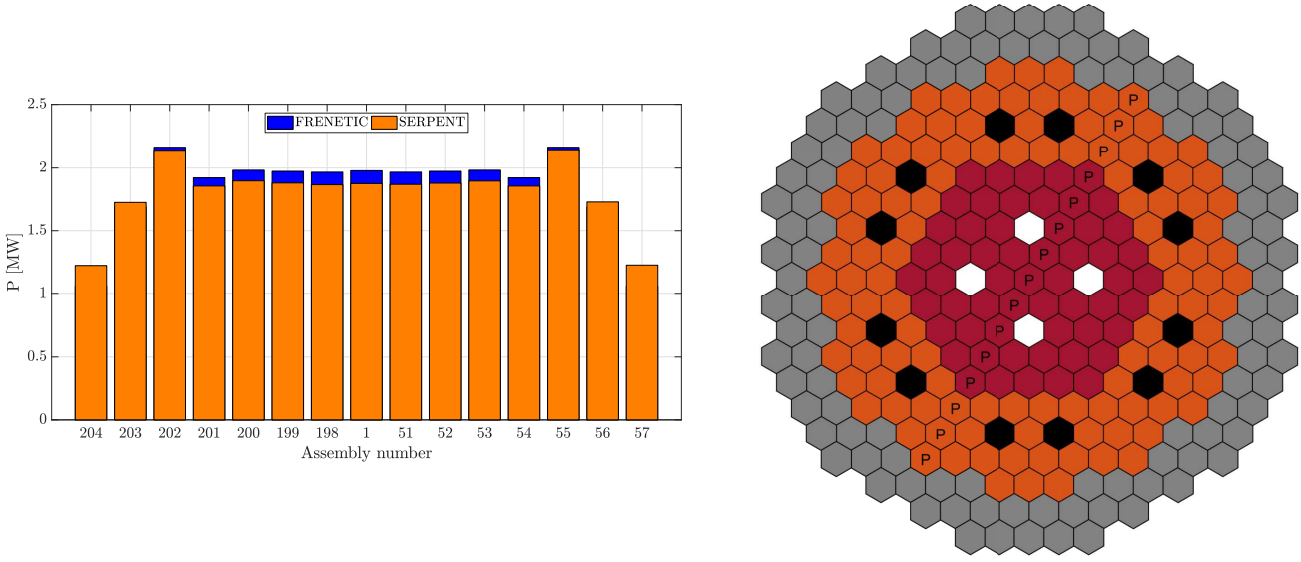

Fig. 13. Comparison between the radial power profile calculated by Serpent and the first FRENETIC model (i.e., without barrel and external lead) for some selected FAs in HZP, i.e., uniform 673 K (left), and radial map of the core with the employed FAs indicated (right). Note the different selection of FAs with respect to Figure 12.

5.2 NE calculations at operational temperature

After the successful neutronic benchmark exercise, a steady-state simulation in multiphysics mode, i.e., by taking into account the NE-TH coupling, has been performed. As already mentioned, the FRENETIC TH module does not consider the temperature variation in the barrel and external lead regions. This allows performing the simulation by taking into account the relevant NE effect associated to the presence of these regions, while neglecting the (much less relevant) associated TH effects.

The FRENETIC run generates the temperature value for each FA at different heights for both the coolant and the fuel. If such information is introduced directly into Serpent, the input file should identify each single mesh used in FRENETIC as a separate universe in Serpent, with its own temperature and composition and the resulting memory requirement would become prohibitive. Therefore, a set of concentric regions has been identified, each characterized by a single temperature value, having verified that the maximum temperature difference between FAs within the same radial region is below 1 K. Axially, all the materials composing the regions below the active zone have been assumed to

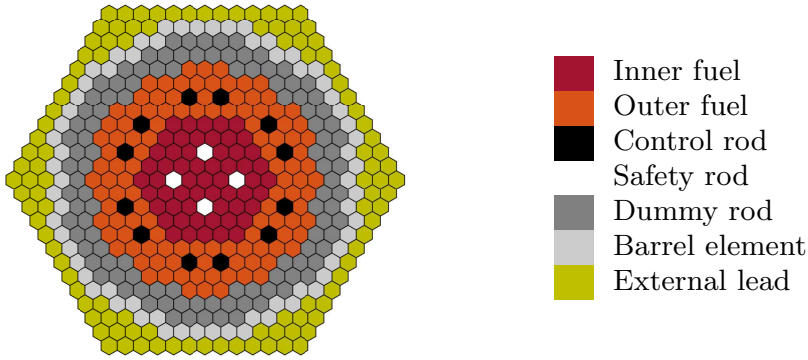

Fig. 14. Radial scheme of the improved FRENETIC model of the ALFRED core (i.e., including barrel and external lead).

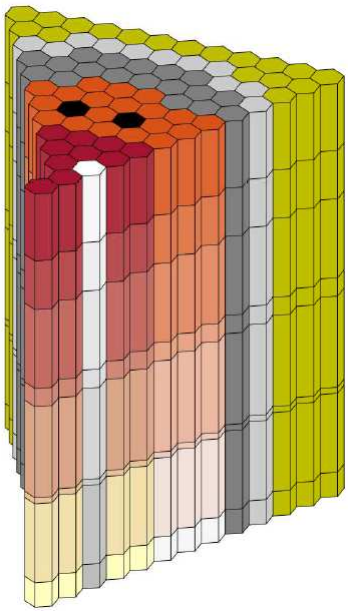

Fig. 15. 3D visualisation of the improved FRENETIC model fo the ALFRED core (i.e., including barrel and external lead).

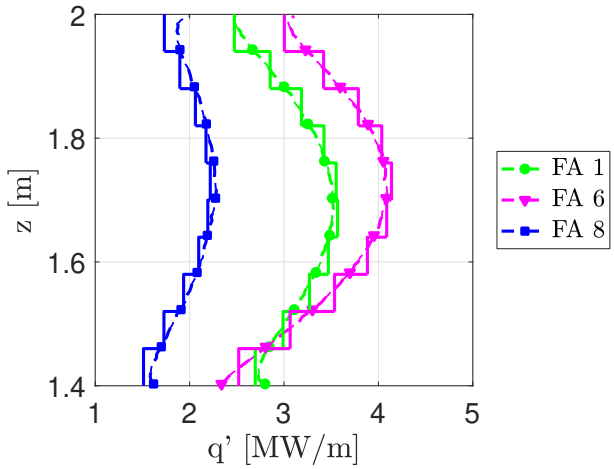

Fig. 16. Comparison between the linear power calculated by Serpent and FRENETIC for three selected FAs (left) in HZP (uniform 673 K). For the identification of the FAs, please refer to Fig. 18.

be at 673 K (i.e., the inlet temperature). Similarly, regions above the active zone share the same temperature, which is equal to the average core outlet temperature. The active region of each FA has instead been subdivided into 10 axial

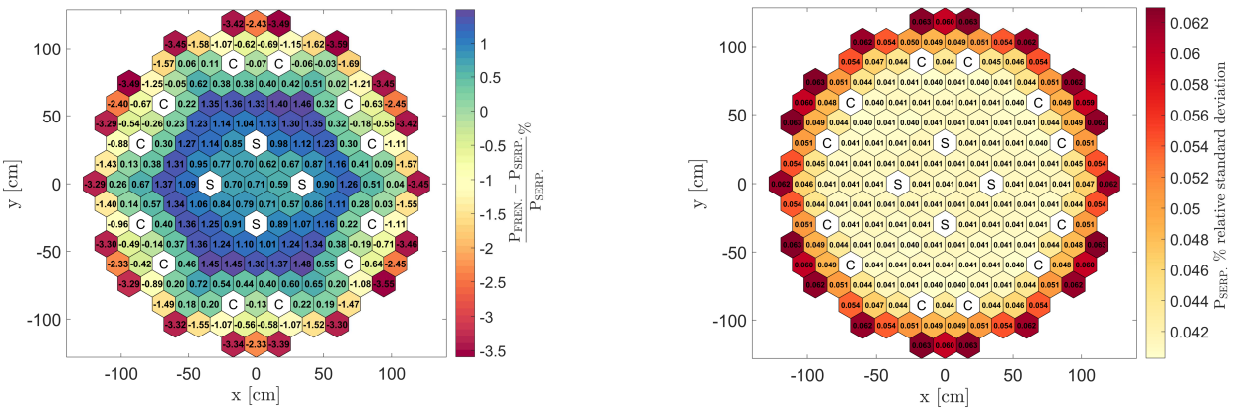

Fig. 17. Percentage relative difference between the power (in MW per FA) computed by Serpent and FRENETIC (left) in HZP (uniform 673 K) and percentage relative standard deviation associated to the power computed by Serpent (right).

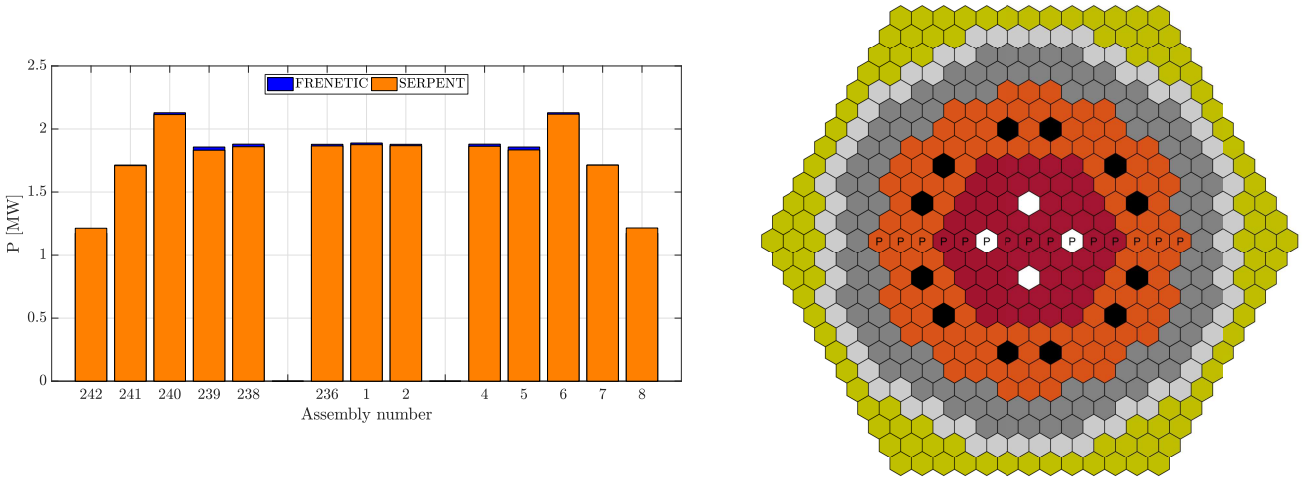

Fig. 18. Comparison between the radial power profile calculated by Serpent and the improved FRENETIC model for some selected FAs in HZP, i.e., uniform 673 K (left) and radial map of the core with the employed FAs indicated (right). The discrepancy between the two calculations is significantly reduced (see Figure 12 for comparison).

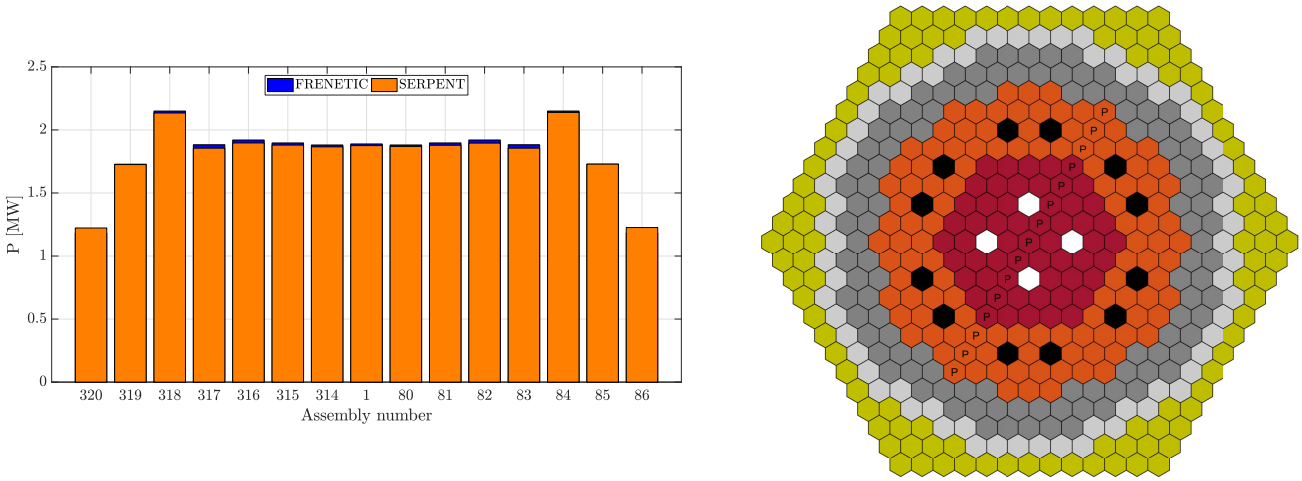

Fig. 19. Comparison between the radial power profile calculated by Serpent and the improved FRENETIC model for some selected FAs in HZP, i.e., uniform 673 K (left) and radial map of the core with the employed FAs indicated (right). The discrepancy between the two calculations is significantly reduced (see Figure 13 for comparison).

segments, each characterized by the corresponding average temperature evaluated by FRENETIC. In this way, a more limited number of regions has been generated, allowing to run a k_{eff} calculation in Serpent with a physically significant temperature distribution. In Figure 20 the radial concentric regions are shown. The multiplication eigenvalue estimated by Serpent is 1.07848 ± 6 pcm, whereas the FRENETIC result is 1.07902 (54 pcm difference), thus further confirming the quality of FRENETIC predictions also in the presence of thermal feedback effects.

Similar comparisons on the power as for the previous cases have been performed. Figure 21 shows the linear power density in three FAs, while the radial distribution is reported in Figures 22 and 23. The relative error on the power for each FA is given in Figure 24, together with Serpent statistical uncertainties.

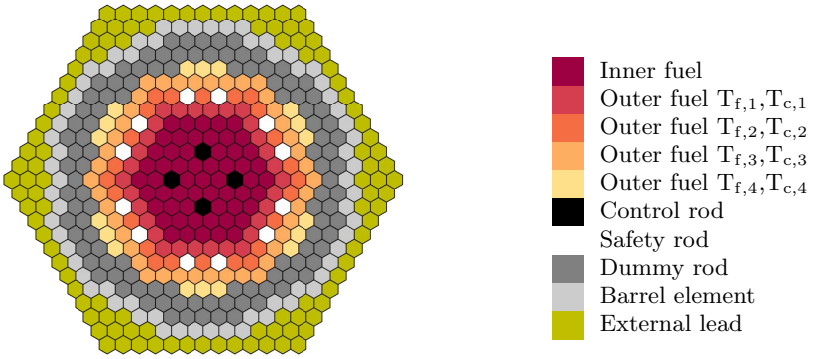

Fig. 20. SERPENT model of the ALFRED core operating in HFP conditions.

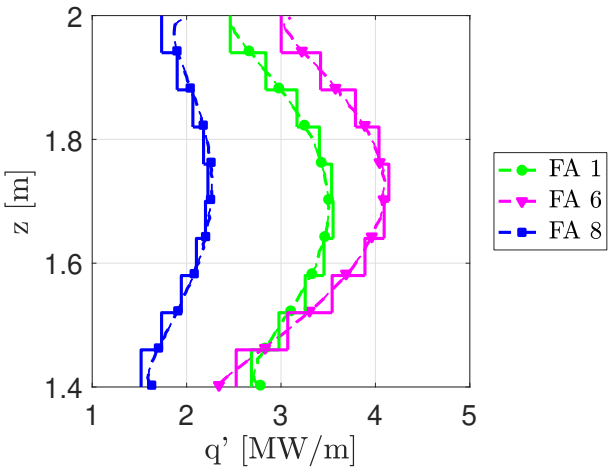

Fig. 21. Comparison between the linear power calculated by Serpent and FRENETIC for three selected FAs in HFP, i.e., using the self-consistently evaluated temperature map. For the identification of the FAs, please refer to Fig. 23.

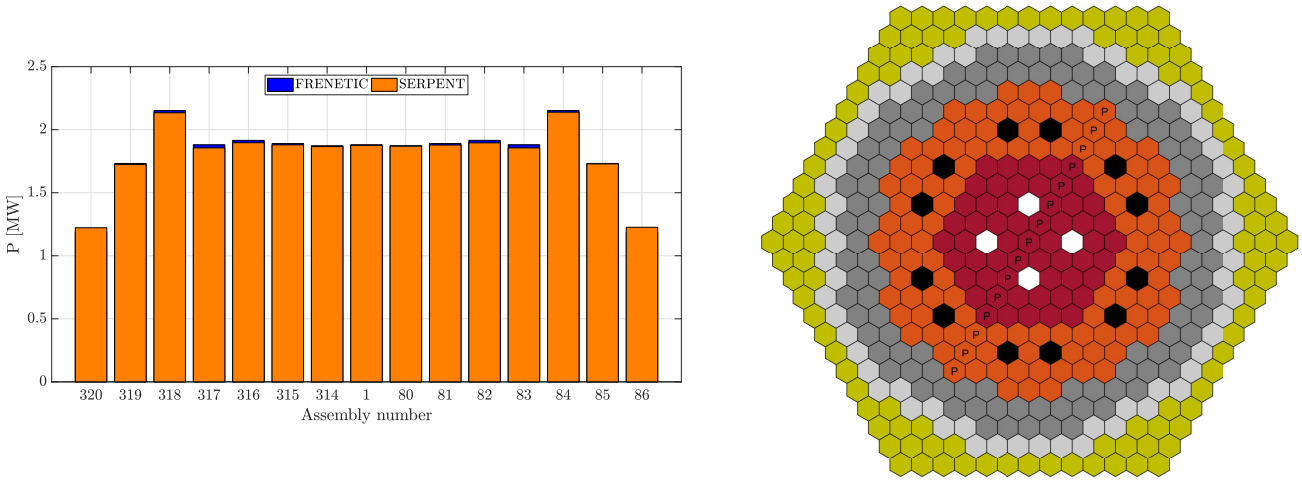

Fig. 22. Comparison between the radial power profile calculated by Serpent and the improved FRENETIC model for some selected FAs in HFP (left) and radial map of the core with the employed FAs indicated (right).

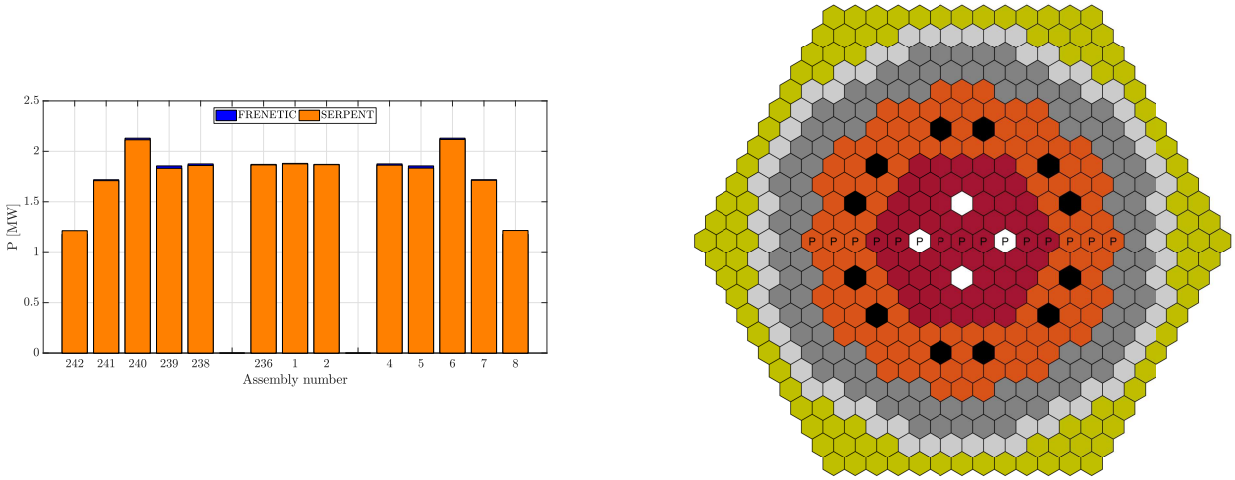

Fig. 23. Comparison between the radial power profile calculated by Serpent and FRENETIC for some selected FAs in HFP (left) and radial map of the core where the FAs are highlighted (right).

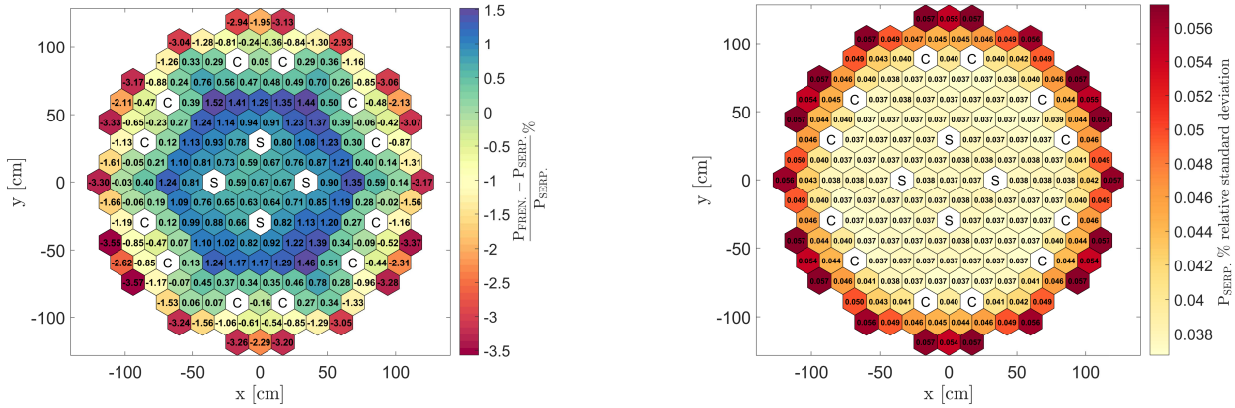

Fig. 24. Percentage relative difference between the assembly-wise power computed by Serpent and FRENETIC in HFP (left) and percentage relative standard deviation associated to the power computed by Serpent (right).

6 Conclusions and perspective

The present work has been focused on the development of an accurate simulation model of the ALFRED core, adopting the Serpent-2 code as reference to be compared to the results of the multiphysics code FRENETIC. The FRENETIC

benchmarking activity in comparison to Serpent has allowed to assess the accuracy of FRENETIC full-core simulations, also highlighting some aspects requiring further R&D work. The optimization of the ALFRED model implemented in FRENETIC has produced satisfactory results, with a significant improvement in the prediction accuracy for what regards neutronic simulations in different thermal conditions, and pointing out the next step to be taken in this perspective. Based on these results, some of the identified further developments are:

- Extension of the TH module in order to allow the simulation of assemblies with stagnating lead in coupled NE-TH mode without resorting to fictitious assemblies;
- Improvement of the energy group structure with more advanced methodologies [13];
- Improvement of the axial representation of the core, starting from the tally definition in Serpent.

In conclusion, we believe that the present state of the FRENETIC code and its associated model for the ALFRED core can provide useful contribution to the analysis of the ALFRED design, performing both steady-state and time-dependent multiphysics simulations of safety relevant scenarios for LFRs.

References

1. R. Bonifetto, S. Dulla, P. Ravetto, L. Savoldi Richard, and R. Zanino. "A full-core coupled neutronic/thermal-hydraulic code for the modeling of lead-cooled nuclear fast reactors." Nuclear Engineering and Design, **volume 261**, pp. 85–94 (2013).
2. D. Caron, R. Bonifetto, S. Dulla, V. Mascolino, P. Ravetto, L. Savoldi, D. Valerio, and R. Zanino. "Full-core coupled neutronic/thermal-hydraulic modelling of the EBR-II SHRT-45R transient." International Journal of Energy Research, **volume 42**(1), pp. 134–150 (2016).
3. D. Caron, S. Dulla, P. Ravetto, L. Savoldi, and R. Zanino. "Models and methods for the representation of decay and photon heat in spatial kinetics calculations." In Proceedings of PHYSOR 2016, pp. 2416–2425. USA (2016).
4. J. Leppänen, M. Pusa, T. Viitanen, V. Valtavirta, and T. Kaltiaisenaho. "The Serpent Monte Carlo code: Status, development and applications in 2013." Annals of Nuclear Energy, **volume 82**, pp. 142–150 (2015).
5. G. Grasso, C. Petrovich, D. Mattioli, C. Artioli, P. Sciora, D. Gugiu, G. Bandini, E. Bubelis, and K. Mikityuk. "The core design of ALFRED, a demonstrator for the European lead-cooled reactors." Nuclear Engineering and Design, **volume 278**, pp. 287–301 (2014).
6. A. Alemberti. "Final Report Summary - LEADER (Lead-cooled European Advanced Demonstration Reactor)." Technical report, CORDIS (Community Research and Development Information Service) (2013).
7. L. Savoldi Richard, F. Casella, B. Fiori, and R. Zanino. "The 4C code forthe cryogenic circuit conductor and coil modeling in ITER." Cryogenics, **volume 50**, pp. 167–176 (2010).
8. R. Bonifetto, R. Zanino, L. Savoldi Richard, and A. Del Nevo. "Benchmark and preliminary validation of the thermal-hydraulic module of the FRENETIC code against EBR-II data." In Proceedings of ATH 2014, Reno, Nevada (2014).
9. R. Zanino, R. Bonifetto, A. Chiampichetti, I. Di Piazza, L. Savoldi, and M. Tarantino. "First validation of the FRENETIC code thermal-hydraulic model against the ENEA integral circulation experiment." Transactions of the American Nuclear Society, **volume 107**, pp. 1395–1398 (2012).
10. G. Rimpault, D. Plisson, J. Tommasi, R. Jacqmin, D. Verrier, and D. Biron. "The ERANOS Code and Data System for Fast Reactor Neutronic Analyses." In Proceedings of PHYSOR 2002 (2002).
11. V. Fabrizio, S. Dulla, M. Nervo, P. Ravetto, G. Bianchini, and V. Peluso. "ALFRED Reactor: evaluation of multi-temperature cross section sets by deterministic and stochastic methods." Technical report, Report RdS/2013/018 (2013).
12. D. Caron. Neutronics methods for the multiphysics analysis of nuclear fission systems. Ph.D. thesis, Politecnico di Torino (2017).
13. M. Massone, F. Gabrielli, and A. Rineiski. "A genetic algorithm for multigroup energy structure search." Annals of Nuclear Energy, **volume 105**, pp. 369–387 (2017).